CRYSTAL GROWTH & DESIGN
2008
VOL. 8, NO. 5
1723–1726

Effect of Stacking Fault on the Formation of the Saw-Teeth of ZnS Nanosaws

Jian Yan,* Zhaoming Wang, and Lide Zhang*

Key Laboratory of Materials Physics, Institute of Solid State Physics, Hefei Institutes of Physical Science, Chinese Academy of Sciences, P.O. Box 1129, Hefei 230031, P.R. China

Received January 12, 2008; Revised Manuscript Received January 22, 2008

ABSTRACT: We report the effect of stacking fault on the formation of the saw-teeth of ZnS nanosaws, which were synthesized by a hydrogen-assisted thermal evaporation method. The stem of ZnS nanosaw grows along the [10$\bar{1}$0] direction and possesses wurtzite (WZ) structure, while the saw-tooth grows along the [111] direction and possesses zinc blende (ZB) and WZ mixed structure. The observation of morphology evolution indicates that the stem and saw-tooth must have formed simultaneously. Detailed structure analysis shows that the stacking faults are crucial to the formation of saw-teeth. The stacking faults can cause phase transformation (WZ → ZB structure). Accordingly, step-like boundaries, which consist of the boundary parallel to the close-packed planes and the perpendicular boundary at the growth front, are forming. The ZB ZnS part on the boundaries serves as the nucleus of the saw-tooth and leads the subsequent growth. A defect inducing growth model is proposed to elucidate the detailed growth process.

Introduction

Comb- and sawlike nanostructures have drawn much attention because of their potential applications, such as for nanosensors, nanotweezers, and lasers.[1–9] Very recently, Wang et al.[10,11] fabricated a nanogenerator with vertically aligned ZnO nanowire arrays that were placed under an essential zigzag electrode. This is a very promising solution for powering nanodevices. A ZnO nanocomb with uniform nanorod arrays on its side and the nanosaw serving as the zigzag electrode are very good candidates for fabricating the one-dimensional nanogenerator. However, to acquire these applications, the nanosaws should be fabricated in a controllable way. Thus, it is necessary to understand the growth mechanism of the nanosaws.

Conventionally, the formation of the nanocombs and nanosaws is explained by a two-step growth model,[3–5] namely, the fast-growth of backbone nanobelt followed by the growth of teeth along the [0001] direction due to its self-catalytic activity. However, Huang et al.[9] found some ZnO nanocombs with the backbone nanobelt growing along the [0001] direction and the teeth growing along the [2$\bar{1}\bar{1}$0] direction. And, the observation of incipient ZnS nanosaws in our experiment indicates that the stem and teeth must have formed simultaneously. These results suggest the possibility of a different growth mechanism. Meanwhile, many groups[1–3,5–7] have found that stacking faults and phase transformation always exist in the nanosaws. Ding et al.[5] considered that the phase transformation might be a factor influencing the formation of the saw-teeth. Kavanagh et al.[7] mentioned that the stacking faults and phase transformation might play an important role in the growth process of the nanosaw. However, the micromechanism of formation of their saw-teeth, especially for the effect of the stacking faults and phase transformation, remains unclear and needs further investigating.

In this paper, we show that the stacking fault can induce the formation of ZnS nanosaws. Detailed structure analysis shows that the stacking fault is intrinsic and can cause the phase transformation (WZ → ZB structure). Accordingly, besides the boundary between WZ and ZB regions parallel to the close-packed planes, a perpendicular boundary forms at the growth front. The ZB ZnS part on thus boundaries serves as the nucleus of the saw-tooth and leads the subsequent growth. The detailed growth process is depicted in a defect inducing growth model. These findings are helpful to the controllable synthesis of sawlike nanostructures.

Experimental Section

The synthesis of the ZnS nanosaws was carried out in a conventional horizontal furnace. Briefly, an alumina tube (outer diameter: 25 mm; length: 80 cm) was mounted horizontally inside a single-zone high temperature resistance furnace. A total of 0.5 g of commercially available ZnS powder (Alfa Aesar, 99.99% purity, metal basis) was used as source materials and placed in the center of the heating area. The Si substrate coated with a 1.5 nm thickness Au film was vertically located downstream of the ZnS powders with a distance of 15 cm (about 750 °C). Before heating, the system was purged with 100 sccm argon (purity: 99.999%) for 1 h to clear O_2, and then, the gas flow was changed to 80 sccm Ar mixed with 1% hydrogen. The furnace was heated to 1000 °C in 8 min and kept at this temperature for 20 min. Consequently, the furnace was heated to 1150 °C in 5 min and kept at this temperature for 20 min with the flow of hydrogen of 10 sccm. After the system was cooled down to room temperature, large-scale white wool-like products were deposited onto the silicon substrate.

The as-synthesized products were characterized using field emission scanning electron microscopy (FESEM, Sirion 200) equipped with an energy dispersive X-ray (EDX) spectroscopy and high resolution transmission electron microscopy (HRTEM, JEOL 2010, operated at 200 kV).

Results and Discussion

The morphologies and compositions of the products were characterized by FESEM. Figure 1a is a low magnification SEM image of the products. It can be seen that a large number of saw-shaped nanostructures are dispersed on silicon substrate. The nanosaws are tapered in width along the growth direction. The average length of nanosaws is about 10 μm. The inset shows that the nanosaws are about 50 nm in thickness. It should be pointed out that there exist thinner nanowires on the tips of some nanosaws (Figure 1b). No Au particle was observed on the tips of nanosaws, implying that the growth of the nanosaws is dominated by vapor-solid (VS) mechanism.[12,13] The chemical compositions of the products were detected by energy dispersive

* Corresponding author. Tel.: +86-5515591465; fax: +86-5515591434; e-mail: yanjian@issp.ac.cn (J.Y.) and Ldzhang@issp.ac.cn (L.Z.).

10.1021/cg800040w CCC: $40.75
Published on Web 03/20/2008

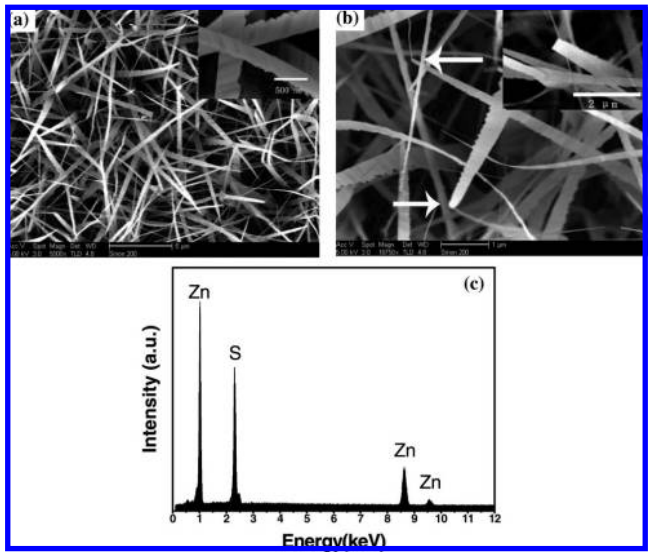

Figure 1. (a) SEM image of ZnS nanosaws and an inset of a high-magnification SEM image; (b) arrows denoting the nanowires growing on the tips of nanosaws and an inset showing a nanosaw without a nanowire growing on its tip; (c) the EDX spectrum of the as-synthesized sample.

X-ray analysis (EDX) equipped on the FESEM. The EDX spectrum (Figure 1c) reveals that nanosaws are composed of the Zn and S with a stoichiometric ratio close to 1:1.

A low magnification TEM image of the nanosaw is shown in Figure 2a. The nanosaw consists of three parts, namely, stem, middle layer, and saw-teeth. Details of microstructure are shown in the HRTEM images (Figure 2b−e) recorded from different regions in Figure 2a. Figure 2b, corresponding to the region marked with black dash rectangle in Figure 2a, shows that the lattice-fringe spacings are 0.63 and 0.33 nm. These lattice-fringe spacings correspond to the (0001) and [10$\bar{1}$0] planes of WZ ZnS, respectively. Therefore, the stem grows along the [10$\bar{1}$0] direction, as shown in Figure 2b. Figure 2c is a HRTEM image taken from the saw-tooth as marked with the black rectangle in Figure 2a. The *d*-spacing of the saw-tooth indicated by parallel lines is 0.31 nm, which corresponds to the distance between the (111) planes of ZB ZnS. The main body of the saw-tooth belongs to the ZB structure (Figure 2c), while there are also some other various structural cells of 2H, 4H and stacking faults (SFs) (Figure 2d). Figure 2d (the region marked with the white rectangle in Figure 2a) shows the boundary between the two saw-teeth. At left of the boundary, there is a series of stacking faults. On the contrary, the part at right of the boundary possesses a ZB structure. It means that there are many Shockley partial dislocations in this region. Figure 2e is the HRTEM image recorded from the region marked by the white dash rectangle in Figure 2a. It displays the boundary between the root of the saw-tooth and the middle layer. The boundary consists of a series of stacking faults which are parallel to the (0001) plane and an extended dislocation (not parallel to (0001) plane). The boundary is in the step-like shape as indicated by the arrows. Here, it is defined as a type A step-like boundary (another kind of step-like boundary will be introduced in the next paragraph). On the top of the step-like boundary (type A), the ZnS possesses ZB structure. The SAED spectrum (Figure 2f), taken from the region marked with white circle in Figure 2a, reflects the characteristics of the complex crystal structure.

After these images were taken from the nanosaw, the sample was illuminated under a 200 kV electron beam for a long time.

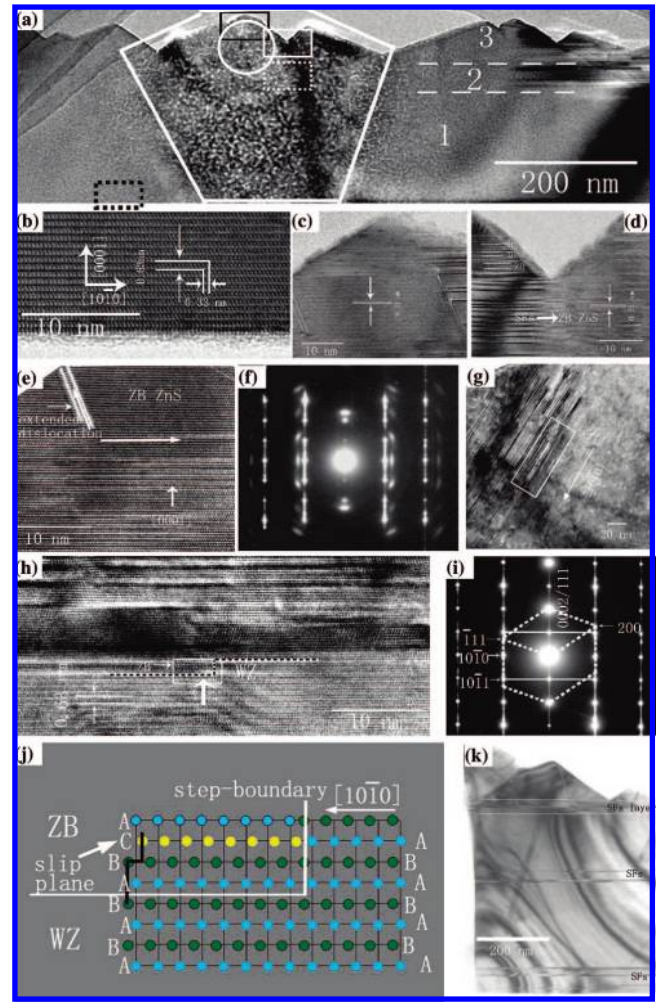

Figure 2. (a) The typical TEM image of a nanosaw after illumination by an electron beam, showing the phase transformation and planar defects as marked with polygon. In the nanosaw, there are three part regions (separated by the white dash lines): stem, middle layer, and saw-teeth as marked with the numbers '1', '2', '3', respectively. The white dash lines are not the exact boundaries of the three regions; (b−e) HRTEM images recorded from the black dash rectangle, black rectangle, white rectangle, and white dash rectangle enclosed regions labeled in (a), respectively; (f) The SAED pattern taken from the white circle region; (g) the TEM image recorded from another nanosaw and the arrow showing the growth direction; (h) The HRTEM image recorded from the rectangle enclosed region labeled in (g); (i) the corresponding SAED pattern; (j) a simple ideal structure model of the region as marked with a rectangle in panel h; (k) a bright field, 2-beam diffraction image of the ZnS nanosaw showing a stacking faults layer (as indicated by two white lines) sandwiched by the stem and saw-teeth.

The phase of ZnS changed as marked with polygon in Figure 2a.[2] The TEM image (Figure 2g) of the interface between the stem and the middle layer was taken from another nanosaw. It is worth pointing out that this nanosaw grows toward left as indicated by the arrow in Figure 2g. Figure 2h is the HRTEM image recorded from the rectangular area in Figure 2g. In the middle layer, the main body has the ZB structure together with many stacking faults, while the stem has the WZ structure. The SAED spectrum (Figure 2i) displays the coexistence of the ZB (dash line) and WZ structures (solid line). An outcrop of stacking fault, namely, the Shockley partial dislocation, is found at the interface as indicated by the arrow in Figure 2h. Careful examination indicates that the stacking fault is intrinsic (type-

II) with the displacement ($\vec{R} = 1/3[0\bar{1}10]$). An intrinsic stacking fault (type-II) transforms the perfect-crystal layer sequence . . .ABABABAB. . . into . . .AB**ABC**ACA. . . . It can be seen that the layer **ABC** has the ZB structure. This is the probable origin of the phase transformation (WZ → ZB structure) in the ZnS nanosaws. It is worth noting that the slip plane is the (0002) plane, so the stacking faults are parallel to the (0002) plane. A simple structure model of this region as marked with a rectangle in Figure 2h is shown in Figure 2j. It can be seen that besides the stacking faults associated with the close-packed planes between the WZ and ZB regions there is also a perpendicular boundary between WZ and ZB phases forming on the WZ [$10\bar{1}0$] plane as indicated by two perpendicular white lines in Figure 2j (or dash lines in Figure 2h). The boundary is also in the step-like shape. Thus, it is also called the step-like boundary as type B. These two kinds of step-like boundaries (type A and type B) can cause three effects. (1) The step-like boundary (type B) shrinks the width of the stem and that is the reason why the observed saw-shaped nanostructures are tapered shape.[5,7] (2) The step-like boundary (type B) produces a substep on the [$10\bar{1}0$] plane as indicated by the black lines in Figure 2j. Ming et al.[14] reported that the two-dimensional heterogeneous nucleation barrier at the substep is always smaller than that of conventional two-dimensional nucleation. Thus, ZnS vapor prefers to nucleate at the substep. At the end of heating in our experiment, the gas supersaturation is low, which benefits the growth of nanowires.[15] So, the nanowires can grow on the tips of nanosaws. It is coincident with the observation of SEM. (3) On top of step-like boundary (type A and type B), ZnS has the ZB structure. This is important to the formation of saw-teeth. It serves as the nucleus of the saw-tooth. Figure 2k, a bright field TEM image of ZnS nanosaw, shows that a stacking faults layer is sandwiched by the WZ stem and ZB saw-teeth. Many stacking faults also exist in the stem, which indicates that the nucleation of stacking faults can easily occur in our case. According to the TEM observations, the stacking faults exist throughout the whole nanosaw. In recent reports,[1–3,5–7] the stacking faults have been found in the nanosaws. Borchers et al.[6] found that the stacking faults have already occurred during nucleation of the nanoribbon. Kavanagh et al.[7] found some stacking faults that are not parallel to the (0001) plane in the WZ ZnSe nanosaws. To our best knowledge, most nanosaws grow along [$10\bar{1}0$,] and the stem has WZ structure, except two kinds of special nanosaws: One is the GaN nanosaw,[1] which grows along the [$10\bar{1}1$] direction, and the other is the ZB ZnSe nanosaw.[7] In these two kinds of nanosaws, the stacking faults have also been found.[1,7] Regardless of the different growth directions and different crystal structures, the stacking faults exist in nanosaws both in previous literature and in our work.

To detect the growth process of ZnS nanosaws, we investigated the morphology of ZnS nanosaws grown in the initial stage. The sample was obtained at a temperature of 1000 °C for 20 min, which consists of a film-like layer of seed-like nanocrystals and a small quantity of nanosaws as shown in Figure 3a. Figure 3b is an enlarged image of the region marked with a rectangle in Figure 3a. The schematic diagram (inset) shows that a half "saw-tooth" marked with a polygon is growing up. It can be inferred that that the stem and teeth must have formed simultaneously. In a recent report,[9] ZnO nanocombs with the backbone nanobelt growing along the [0001] direction and the teeth growing along the [$2\bar{1}\bar{1}0$] direction have been found. These results suggest that besides the polar surface[3–5] other factors can also induce the growth of the nanocombs or the nanosaws. There is the possibility of a different growth

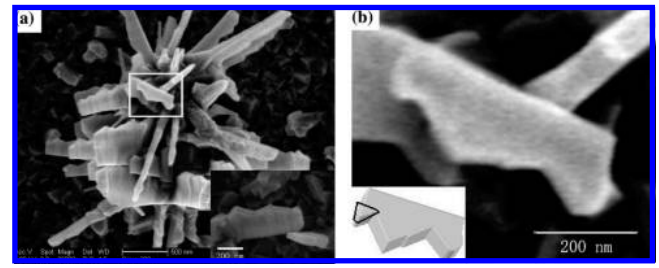

Figure 3. (a) The SEM image of incipient nanosaws. The nanosaws grow from one site, while the inset shows a nanosaw growing from one seed. (b) The enlarged image of the area marked with a rectangle in (a) and the inset being the sketch map of the nanosaw showing a half "saw-tooth".

mechanism. In addition, based on the HRTEM analysis, the stacking faults exist in the whole nanosaw. It is reasonable to speculate that the stacking faults form continuously with the growth of the stem.

When the peak temperature is lowered or raised (1000, 1100, 1200 °C), ZnS nanosaws can also be obtained in the deposition zone (700−800 °C). However, if the hydrogen gas is removed, the sample is dominated by a large number of WZ ZnS nanoribbons and nanowires, and only a few ZnS nanosaws were found. These experimental results suggest that the hydrogen gas is very important to the formation of ZnS nanosaws. Alhough the effect of hydrogen is unclear, one possibility is that the hydrogen gas is related to the nucleation of stacking faults. In the case of ZnS, the stacking fault energy and transformation energy (WZ → ZB structure) are both low.[6] Thus, the stacking fault and phase transformation can easily occur. In the presence of hydrogen, the ZnS gas supersaturation is high, which can induce stacking faults.[16,17] As analyzed above, the ZB structured ZnS can be induced by the stacking fault. Furthermore, recent reports[3,18] indicate that lower deposition temperature (680−750 °C) is advantageous to the formation of ZB ZnS. In our case, the deposition temperature is around 750 °C. Thus, the ZB ZnS part caused by the stacking fault can remain stable and serve as the nucleus of the saw-tooth. If the hydrogen gas is removed, the ZnS gas supersaturation is much lower. It cannot easily cause the stacking faults. Therefore, ZnS nanosaws cannot be acquired in large scale.

According to the above results and analysis, a defect inducing growth model of ZnS nanosaws is proposed based on the basic point that the stacking faults form continuously with the growth of the stem. The formation of saw-teeth is elucidated as follows (Figure 4): With the temperature rising to 1150 °C, nanoribbon (stage 2) begins to grow out of the seed (stage 1) along the [$10\bar{1}0$] direction. ZnS vapor pressure is high under the presence of hydrogen,[16] and the stacking faults are induced.[17] Namely, the step-like boundary (type B) is generated (stage 3). Subsequently, the ZB ZnS part on the step-like boundary serves as the nucleus. During the further growth stage, the growth front (the (111) plane) of the nucleus has a fast growth rate, and will minimize in area.[19] It leads the nucleus to a triangular shape, and namely, the saw-tooth forms (stage 4). When the second step-like boundary (type B) forms, a region (baby blue area, stage 5) with stress appears due to the mismatch of stacking sequence between the atomic layers (black area, stage 5) on the first step-like boundary and that (gray area, stage 5) on the second step-like boundary. The stress increases both along [$10\bar{1}0$] and [0001] during subsequent growth. With the stress getting to a certain grade, a middle layer with stacking faults, other defects (e.g., extended dislocation) and phase transforma-

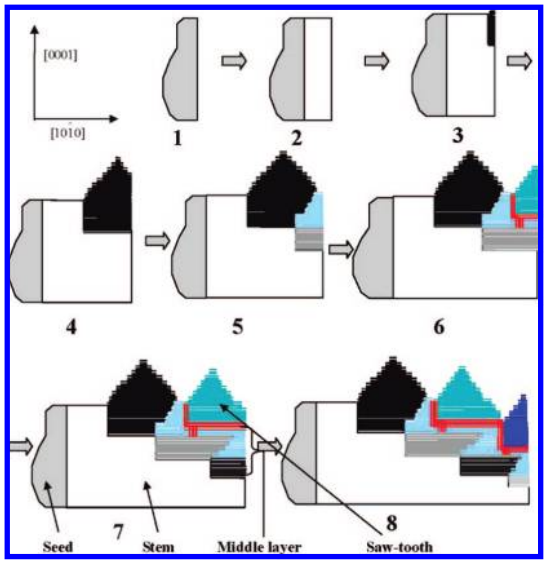

Figure 4. The schematic diagram of the growth process of ZnS nanosaws; see text for details. Two arrows show the [10$\bar{1}$0] and (0001] directions, respectively.

tion form to reduce the additional system energy.[20] Accordingly, a step-like boundary (type A, red area, stage 6) is generated by the stacking faults and the other defects. The ZB ZnS part on the step-like boundary (type A) leads the growth of the second saw-tooth (stage 6–7). Meanwhile, the step-like boundary (type A) prevents the lateral growth of the first saw-tooth. Stage 8 shows the formation of the third saw-tooth and more saw-teeth will form in sequence. It can be seen that the stacking faults play a key role during the growth process of the saw-teeth. The saw-tooth grows on the step-like boundary as shown in Figure 4.

Conclusions

In summary, this work provides a deep understanding of the growth mechanism of ZnS nanosaws synthesized in large scale by the hydrogen-assisted thermal evaporation method. This paper shows that the saw-tooth and stem have formed simultaneously. The intrinsic stacking faults are important to the formation of saw-tooth. It can cause the phase transformation (WZ → ZB structure) in the WZ stem. Accordingly, step-like boundaries are forming. The ZB ZnS part on the step-like boundary serves as the nucleus and leads the subsequent growth of the saw-tooth. Our results show that the stacking fault is an important factor in controlling the morphology of nanostructures. It is also worth noting that the hydrogen gas plays an important role in the synthesis of ZnS nanosaws. The synthesized ZnS nanosaws provide a new building block in the future of functional nanodevices.

Acknowledgment. This work was financially supported by the National Major Project of Fundamental Research: Nanomaterials and Nanostructures (Grant No. 2005CB23603), the Special fund for President Scholarship, Chinese Academy of Science and the Natural Science Foundation of China (Grant No. 90406008).

References

(1) Bae, S. Y.; Seo, H. W.; Park, J.; Yang, H. *Chem. Phys. Lett.* **2003**, *373*, 620.
(2) Ma, C.; Moore, D.; Li, J.; Wang, Z. L. *Adv. Mater.* **2003**, *15*, 228.
(3) Ding, Y.; Wang, X. D.; Wang, Z. L. *Chem. Phys. Lett.* **2004**, *398*, 32.
(4) Wang, Z. L.; Kong, X. Y.; Zuo, J. M. *Phys. Rev. Lett.* **2003**, *91*, 185502.
(5) Ding, Y.; Ma, C.; Wang, Z. L. *Adv. Mater.* **2004**, *16*, 1740.
(6) Borchers, C.; Stichtenoth, D.; Muller, S.; Schwen, D.; Ronning, C. *Nanotechnology* **2006**, *17*, 1067.
(7) Wang, Y. Q.; Philipose, U.; Ruda, H.; Kavanagh, K. L. *J. Mater Sci. Mater. Electron.* **2006**, *17*, 1065.
(8) Yan, H. Q.; He, R. R.; Johnson, J.; Law, M.; Saykally, R. J.; Yang, P. D. *J. Am. Chem. Soc.* **2003**, *125*, 4728.
(9) Huang, Y. H.; Zhang, Y.; He, J.; Dai, Y.; Gu, Y. S.; Ji, Z.; Zhou, C. *Ceram. Int.* **2006**, *32*, 561.
(10) Wang, Z. L.; Song, J. H. *Science* **2006**, *312*, 242.
(11) Wang, X. D.; Song, J. H.; Liu, J.; Wang, Z. L. *Science* **2007**, *316*, 102.
(12) Burton, W. K.; Cabrera, N.; Frank, F. C. *Nature* **1949**, *163*, 398.
(13) Yang, P.; Lieber, C. M. *Science* **1997**, *273*, 1836.
(14) Ming, N. B.; Tsukamoto, K.; Sunagawa, I. *J. Cryst. Growth* **1988**, *91*, 11.
(15) Ye, C. H.; Fang, X. S.; Hao, Y. F.; Teng, X. M.; Zhang, L. D. *J. Phys. Chem. B* **2005**, *109*, 19758.
(16) Jiang, Y.; Meng, X. M.; Liu, J.; Xie, Z. Y.; Lee, C. S.; Lee, S. T. *Adv. Mater.* **2003**, *15*, 323.
(17) Yao, N. Z. In *Foundation of Crystal Growth*; University of Science and Technology of China Press: Hefei, 1995; *Chapter 10*, pp 459–461. (in Chinese).
(18) Hu, J. T.; Wang, G. Z.; Guo, C. X.; Li, D. P.; Zhang, L. L.; Zhao, J. J. *J. Lumin.* **2007**, *122–123*, 172.
(19) Donnay, J. D. H.; Harker, D. *Am. Mineral.* **1937**, *22*, 463.
(20) Li, Q.; Gong, X. G.; Wang, C. R.; Wang, J.; Ip, K.; Hark, S. *Adv. Mater.* **2004**, *16*, 1436.

CG800040W